RSC Mechanochemistry

Accepted Manuscript

Published on 12 August 2026

This is an Accepted Manuscript, which has been through the Royal Society of Chemistry peer review process and has been accepted for publication.

Accepted Manuscripts are published online shortly after acceptance, before technical editing, formatting and proof reading. Using this free service, authors can make their results available to the community, in citable form, before we publish the edited article. We will replace this Accepted Manuscript with the edited and formatted Advance Article as soon as it is available.

You can find more information about Accepted Manuscripts in the Information for Authors.

Please note that technical editing may introduce minor changes to the text and/or graphics, which may alter content. The journal's standard Terms & Conditions and the Ethical guidelines still apply. In no event shall the Royal Society of Chemistry be held responsible for any errors or omissions in this Accepted Manuscript or any consequences arising from the use of any information it contains.

ROYAL SOCIETY OF CHEMISTRY

ARTICLE

Mechanochemical One-Pot Synthesis of Fe(II) Schiff-Base Complexes Exhibiting Spin Crossover

Received 00th January 20xx,
Accepted 00th January 20xx

DOI: 10.1039/x0xx00000x

Yolanda Sabater-Algarra,[a§] Catherine G. Dunsford,[a§] Foramben Prajapati,[b] Almudena Inchausti,[b] Patrick Rosa,[b] Helena J. Shepherd*[a]

Spin crossover (SCO) compounds, can reversibly switch between low-spin and high-spin states in response to external stimuli such as temperature, pressure, or light. These transitions involve pronounced changes in magnetic, optical, and structural properties. Consequently, SCO materials are attractive candidates for molecular switches and have recently gained attention as promising solid-state barocaloric cooling materials due to their large and reversible entropy changes. In this context, SCO systems offer a promising, viable, and sustainable solution for next-generation solid-state cooling technologies. The development of environmentally benign technologies must be accompanied by equally sustainable synthetic methodologies. To enable large-scale production and practical implementation, mechanochemistry has emerged as a green approach that minimizes solvent use, reduces reaction times, and facilitates scalability. Here, we investigate the mechanochemical synthesis of three Fe(II) Schiff-base complexes featuring N_4O_2 coordination spheres. Reaction parameters and conditions have been optimised, and all three complexes were successfully synthesised via a one-pot mechanochemical route. The mechanochemically obtained materials closely match those produced by conventional solution-phase methods and retain their characteristic SCO behavior. Two compounds exhibit abrupt spin transitions near room temperature, while the third shows a more gradual transition. Comprehensive characterization was performed using powder X-ray diffraction (PXRD), differential scanning calorimetry (DSC), thermogravimetric analysis (TGA), and vibrating sample magnetometry (VSM). Overall, these results highlight mechanochemistry as a viable and environmentally friendly strategy for screening and producing new promising SCO materials for barocaloric applications, providing a solid foundation for the development of sustainable solid-state refrigeration technologies.

Introduction

Spin crossover (SCO) compounds are molecular switches that can reversibly change their spin state in response to external stimuli such as pressure, light, temperature, magnetic or electric fields, or combinations thereof.[1–5] Although complexes of all first-row d^4–d^7 metal ions have been investigated for their SCO properties,[6–9] Fe(II)-based compounds remain the most extensively studied.[10–12] Their unique behaviour makes SCO materials highly attractive for applications in molecular switches, actuator devices, molecular-based spintronic devices, and hybrid multifunctional materials.[13–16]

SCO systems have recently attracted increasing interest in the field of barocaloric materials,[17–19] since the spin-state change is associated not only with a large volume variation but also with substantial changes in entropy. In this context, materials exhibiting abrupt SCO (spin transition) temperatures close to, but below, room temperature and displaying negligible hysteresis loops are particularly promising candidates for such barocaloric applications. Owing to their ease of structural modification achieved simply by employing different aldehydes and amine/hydrazone starting materials, Schiff-base ligands provide a versatile platform for the design of new SCO complexes. Many such Schiff-base complexes have been shown to exhibit first order SCO near room temperature;[20–24] therefore, they are ideal candidates for exploring their barocaloric properties. Nevertheless, competitive credible candidates for real life barocaloric refrigeration will need to be not only economically competitive but also sustainably synthesizable, to comply with current political objectives for the economy transition towards sustainability (see e.g. the 2020 "New Industrial Strategy for Europe").[25] In this context, the present work explores mechanochemistry as an economically competitive, greener and more sustainable synthetic route to solution-based synthesis, aiming to minimise energy input, solvent consumption, and the number of synthetic steps through efficient one-pot strategies.

Previous studies have demonstrated the successful application of mechanochemistry to the synthesis of SCO materials, in which the magnetic properties retain comparable

[a]*Supramolecular, Interfacial & Synthetic Chemistry Group, School of Natural Sciences, University of Kent, Canterbury CT2 7NH, UK. Email: h.j.shepherd@kent.ac.uk*
[b]*Univ. Bordeaux, CNRS, Bordeaux INP, ICMCB, UMR 5026, F-33600 Pessac, France.*
§ YSA and CGD contributed equally to this work and share first authorship

† Electronic supplementary information (ESI) available: This includes experimental details as well as additional characterization and calorimetric data.

characteristics to their solution-state analogues.[26] In some of these systems, mechanochemistry has been shown to influence the SCO behaviour, particularly in terms of hysteresis width and transition "smoothness" (defined generally as ΔT_{80}, that the difference in the temperatures for which 80% and 20% of the molecular complexes are in high-spin (HS) state).[27] However, in all previous cases, the SCO materials were synthesised from metal salts and commercially available ligands. The one-pot mechanochemical approach presented here has not been reported for SCO systems. This one-pot approach, in which the Schiff-base ligands and SCO complex are formed in the same synthetic step reduces synthetic complexity, involving grinding of the metal salt and ligand precursors simultaneously. One-pot synthesis of metal complexes bearing Schiff-base ligands has been demonstrated for several systems based on Co(II),[28] or with imine-based ligands with Cu(I), and Fe(II).[29] Nevertheless, the retention of their magnetic and caloric properties has not been discussed yet.

To demonstrate the reliability and versatility of this approach, we selected three complexes based on previously reported Schiff bases. These compounds, when prepared by conventional solution-state synthesis, typically form solvated materials that require desolvation in order to exhibit the desired SCO transitions near room temperature.[20–22] It is noteworthy that this desolvation step usually has consequences on the compounds crystallinity and very often accordingly upon the SCO cooperativity, with potential effects on its abruptness and completeness. We report here the mechanochemical synthesis of three tridentate Fe(II) Schiff-base complexes, **Fe(L1)$_2$**, **Fe(L2)$_2$** and **Fe(L3)$_2$** (L1: 4-hydroxy-*N*'-(pyridin-2-ylmethylene)-benzohydrazide; L2: 1-((quinolin-8-ylimino)methyl)naphthalen-2-ol, referred to in the literature as Hqnal; L3: 4-chloro-2-((quinolin-8-ylimino)methyl)phenol, referred to in the literature as 4Cl-qsal, **Scheme 1**), obtained via liquid-assisted grinding (LAG). All complexes are produced quantitatively and retain both their structural phases and magnetic behaviour when compared with their solution-synthesised analogues once desolvated. This strategy thus provides a robust, direct and sustainable route for the preparation of solvent-sensitive Fe(II) SCO complexes, contributing to the development of environmentally responsible barocaloric materials and supporting the broader goals of circularity and reduced carbon footprint in functional materials chemistry.

Results and Discussion

Parameter optimisation for the synthesis of "one-pot" complexes

The first step in optimising the synthetic conditions was to establish a robust and transferable protocol applicable to the broader family of Schiff-base Fe(II) complexes, using **Fe(L1)$_2$** as a model system. Several key parameters were therefore evaluated prior to defining the final conditions.

Base selection

An essential requirement for successful complex formation is the deprotonation of the ligand to enable coordination to the metal centre. Although mechanochemistry is widely used in synthesis, reports specifically addressing mechanochemical deprotonation remain scarce.[28] Potassium carbonate (K_2CO_3) was selected based on previous successful applications in mechanochemical reactions, including the deprotonation of imide functionalities with reactivity comparable to hydrazone fragments. Most importantly, it offers advantages in terms of low cost and low toxicity.[30,31]

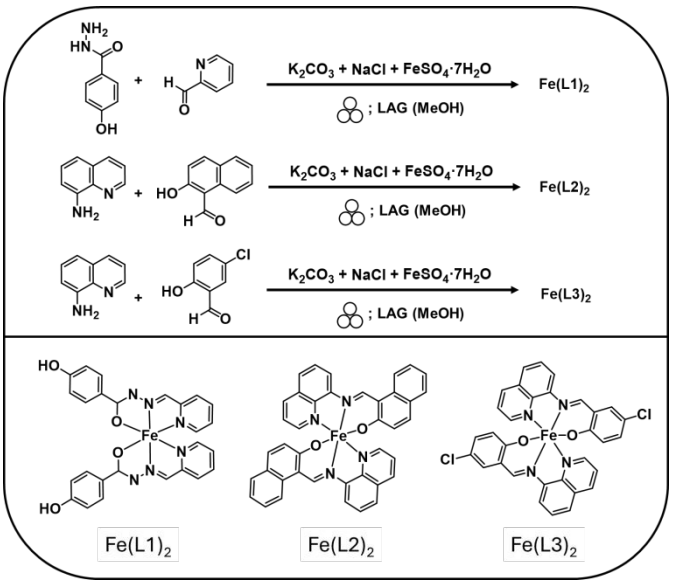

Scheme 1. Mechanochemical one-pot process for the synthesis and chemical structure for **Fe(L1)$_2$**, **Fe(L2)$_2$** and **Fe(L3)$_2$**.

Grinding auxiliary

During the in-situ formation of the Schiff-base ligand, water generated in the condensation step led to poor rheological

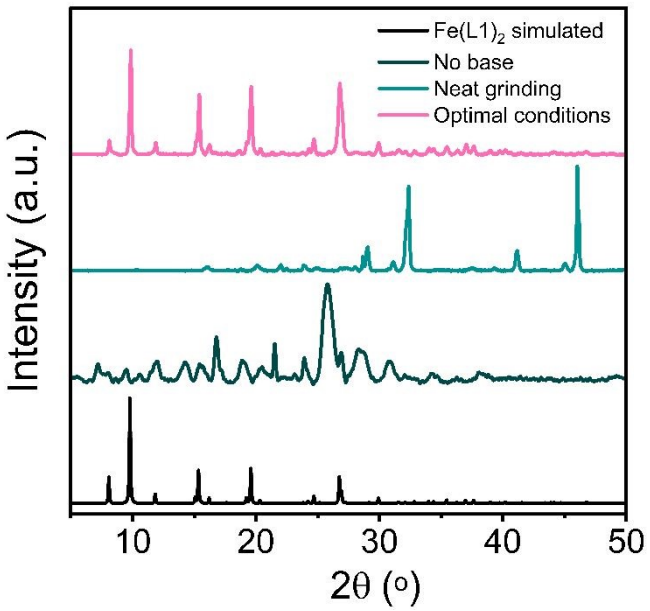

Figure 1. PXRD pattern comparison for **Fe(L1)$_2$**: from top to bottom, simulated (black) from reference 20, and synthesised in absence of base (dark green), neat grinding (green) and with the optimal conditions (pink).

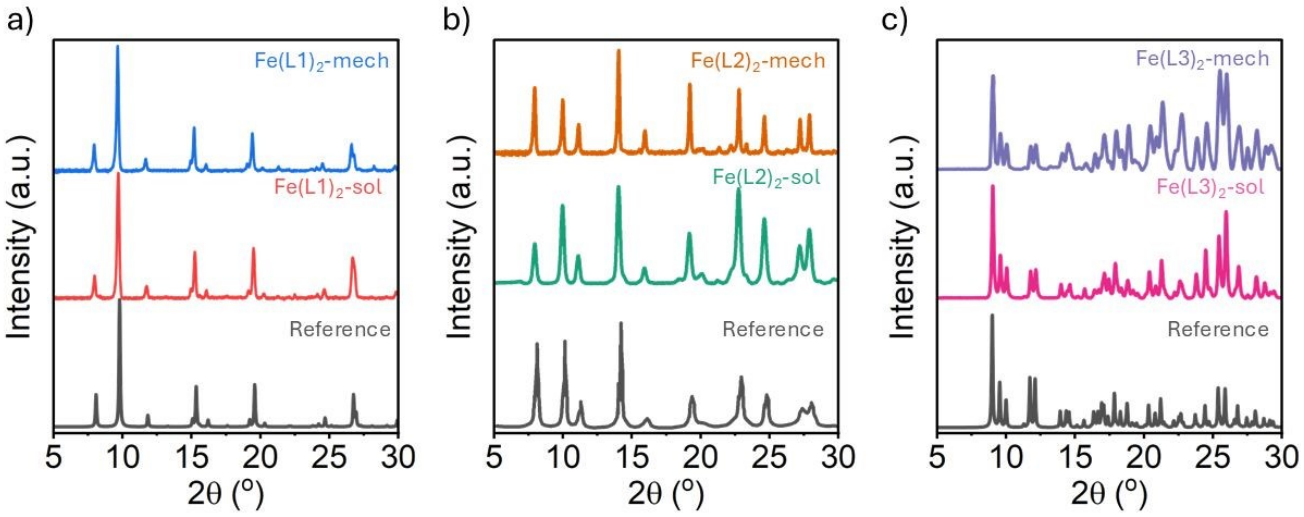

Figure 2. PXRD patterns of the samples synthesised by a mechanochemical one-pot process (top) and solution-state (middle) of **Fe(L1)₂** (a), **Fe(L2)₂** (b) and **Fe(L3)₂** (c) and compared with the simulated pattern from the crystalline structure (bottom), adapted from references 20, 21 and 24.

behaviour, producing a viscous mixture that hindered efficient grinding. As **Fe(L1)₂** is insoluble in water, its presence did not promote the reaction, and small amounts of methanol were insufficient to restore proper mixing. To overcome this limitation, sodium chloride was introduced as a grinding auxiliary and used in excess (5 equivalents),[32,33] effectively preventing agglomeration and improving sample homogeneity.

Neat grinding versus liquid-assisted grinding (LAG)

Three different experiments were performed using a high-speed, dual-axis centrifugal mixing device for 10 minutes: (1) milling of the starting materials (hydrazone, aldehyde, and iron salt precursor) with NaCl as grinding auxiliary and liquid-assisted grinding (LAG) using methanol (η = 0.5 µL·mg^{-1}, where η is the ratio of liquid volume to the mass of solids); (2) neat grinding of the starting materials with NaCl and K_2CO_3, in the absence of solvent; and (3) the same conditions as in (2), but with the addition of methanol for LAG (η = 0.5 µL·mg^{-1}).

Powder X-ray diffraction (PXRD) was performed on each sample (**Figure 1**). The diffraction patterns revealed that neither the solvent-free reaction nor the base-free variation led to the formation of **Fe(L1)₂**, indicating the formation of side products rather than the desired compound, thus demonstrating that optimal conditions require the use of a base, a grinding auxiliary, and LAG. Additionally, images of the obtained compounds are provided to illustrate that color differences can serve as a simple visual indicator of reaction progress (see Figure S1).

Liquid-assisted grinding (LAG) vs. solution-state synthesis

The following mechanochemical one-pot procedure was applied for the synthesis of **Fe(L1)₂-mech,** and has been used analogously for all other complexes. 4-Hydroxybenzohydrazide, 2-pyridinecarboxaldehyde, K_2CO_3, NaCl, and $FeSO_4{\cdot}7H_2O$ were mixed in 2:2:2:1:0.9 ratio with four stainless steel balls at 3500 rpm in a SpeedMixer for 10 minutes in the presence of MeOH. After mixing, a green paste was obtained, which was washed with water, filtered, and dried under vacuum. Once the synthetic procedure was established, the same methodology was applied to the preparation of **Fe(L2)₂** and **Fe(L3)₂**.

For all three mechanochemically-prepared compounds (**Fe(L1)₂-mech, Fe(L2)₂-mech** and **Fe(L3)₂-mech**) synthesised, their structural features and chemical composition were compared with their solution-state analogues using analytical techniques, including Fourier-transform infrared spectroscopy (FT-IR), elemental analysis (EA), Inductively Coupled Plasma Optical Emission Spectroscopy (ICP-OES) and thermogravimetric analysis (TGA). FT-IR confirms that all characteristic bands of the compounds in the molecular fingerprint region are preserved in both preparation methods for all three cases, with only subtle differences in relative band intensities (see Figs. S2 to S4 in ESI). Combined EA and ICP-OES results agree with the expected chemical formulas for all compounds, despite minor NaCl and K_2SO_4 residues remaining after washing and filtration, which do not affect their functionalities. The results and calculated formulae are provided in the ESI. Regarding thermal stability, the onset temperature of the first decomposition step is similar for compounds obtained by both methods and is even slightly higher for the mechanochemically prepared samples (see Figs. S5 to S7 in ESI).

Examination of the PXRD patterns of the materials obtained both *via* solution synthesis and the one-pot mechanochemical approach shows that the positions and relative intensities of the diffraction peaks are in excellent agreement with those predicted from the unsolvated crystal structures (**Figure 2a–c**). These results highlight the clear advantages of the mechanochemical method over traditional solution-state synthesis. The solution-based approach typically involves multiple steps, including ligand synthesis under solvothermal conditions (e.g., L1 requires 24 h at 65 °C using 20 mL of solvent per gram of starting material),[34] followed by ligand isolation, complex formation in a separate step, and a final desolvation

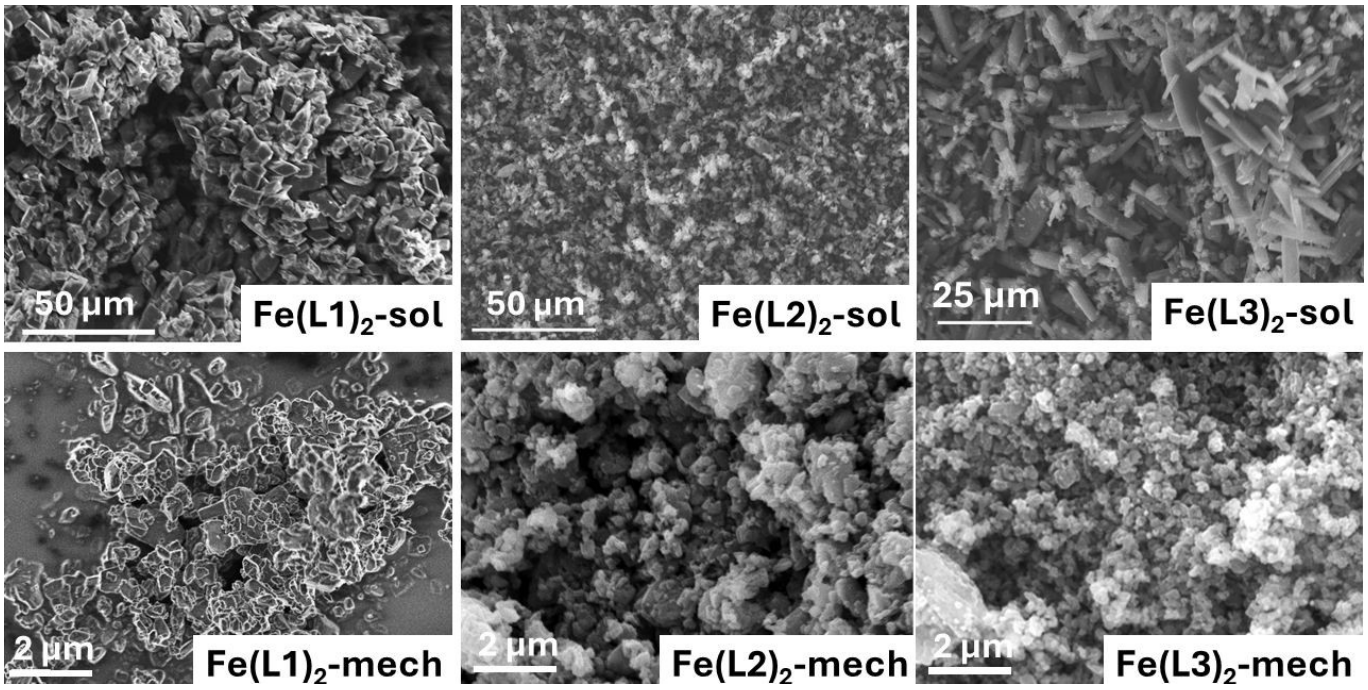

Figure 3. SEM images of **Fe(L1)$_2$**, **Fe(L2)$_2$**, and **Fe(L3)$_2$** compounds prepared by the solution-state method (top row) and the one-pot mechanochemical method (bottom row).

process. Moreover, the synthesis of the complex in solution requires degassed solvents and an inert atmosphere to prevent oxidation to Fe(III), further increasing experimental complexity. The subsequent desolvation step may also damage the crystals and compromise the material quality.

In contrast, mechanochemistry enables a genuine one-pot process in which the ligand is formed *in situ*, eliminating the need for intermediate isolation steps prior to complex formation. The unsolvated complex is obtained directly in good yields, while avoiding the use of degassed solvents and inert atmospheres, as well as preventing crystal damage associated with post-synthetic desolvation. The full PXRD range is provided in the ESI (Figures S8–S10).

To gain insight into the reaction mechanism, *ex situ* FT-IR and PXRD experiments were performed by analysing samples collected at different reaction times. The FT-IR results reveal that ligand formation occurs extremely rapidly. The aldehyde C=O band disappears within the first 30 s, while the characteristic C=N stretching bands of the deprotonated hydrazone appear simultaneously, indicating fast condensation and deprotonation. Weak N–H stretching bands, assigned to the free hydrazone intermediate, are only detected during the first 1.5 min, suggesting that ligand formation is complete at this stage. In contrast, the *ex-situ* PXRD patterns show a more gradual structural evolution. Although diffraction peaks corresponding to the SCO-active phase of the coordination compound become evident after 3–5 min, weak reflections from the starting materials remain until complete conversion is reached after approximately 10 min. Together, these results support a stepwise reaction mechanism involving rapid hydrazone formation, followed by deprotonation and subsequent coordination to the metal centre, with crystal structure assembly representing the rate-limiting step (Figures S11-S14).

To further support the sustainability of our methodology, the E-factor and Process Mass Intensity (PMI)[35] were calculated for the three compounds synthesized by mechanochemistry and compared with those obtained using the corresponding solution-based protocols. Both metrics were calculated assuming identical solvent consumption during the work-up stage for the two methodologies. Detailed calculations and complete datasets are provided in the Supporting Information. The PMI decreased from 138 (solution) to 85 (one-pot) for **Fe(L1)$_2$**, from 195 (solution) to 60 (one-pot) for **Fe(L2)$_2$**, and from 125 (solution) to 57 (one-pot) for **Fe(L3)$_2$**, while the corresponding E-factor decreased from 137 to 84, 194 to 59, and 124 to 56, respectively. These results clearly demonstrate the improved sustainability of the mechanochemical protocol, primarily due to the substantial reduction in solvent consumption during the synthetic steps, leading to lower material usage and waste generation.

Analysis of morphology and particle size

Given the different nature of the synthetic approaches, scanning electron microscopy (SEM) was employed to examine the particle shape, morphology, and size of the materials obtained by each method, allowing a direct comparison between solution-state and mechanochemical syntheses (see Figs. S15 to S20 in ESI for size distribution histograms). **Figure 3** illustrates how the synthesis method influences particle characteristics across the three complexes. Solution-state samples show larger and more regular crystallite formation. **Fe(L1)$_2$-sol** and **Fe(L2)$_2$-sol** display well-defined plate-like crystallite morphology whereas **Fe(L3)$_2$-sol** presents elongated

rod-like crystals. For solution-state samples, particle size and dispersity were determined by scanning electron microscopy (SEM), revealing crystallites are on the order of 10 µm. In contrast, their mechanochemical counterparts appear irregular and less uniform, exhibiting smaller and more fragmented particles, consistent with mechanical grinding and limited crystal growth. For the mechanochemically prepared samples, SEM was employed to obtain a rough estimate of the particle size, with representative images shown in **Figure 3**. These samples exhibit a broader particle size distribution than those prepared by solution-state; however, their average particle size is approximately two orders of magnitude smaller, falling in the range of hundreds of nanometres. Table 1 summarises the particle sizes and morphologies of all the samples.

Table 1. Table of particle sizes measured by the Scherrer equation, with SEM sizes and shapes determined from SEM micrographs.

	SEM	
	Particle size (µm)	**Shape**
Fe(L1)$_2$-sol	9.5 ± 1.8	Plate
Fe(L2)$_2$-sol	2.9 ± 0.9	Plate
Fe(L3)$_2$-sol	11.6 ± 5.2	Rod
	Particle size (nm)	**Shape**
Fe(L1)$_2$-mech	274 ± 21	Irregular
Fe(L2)$_2$-mech	364 ± 98	Irregular
Fe(L3)$_2$-mech	509 ± 128	Irregular

Retention of the magnetic properties

Particle size, morphology and crystallinity have all previously been shown to affect SCO properties.[36–38] While PXRD confirms that the one-pot synthesis yields the same crystalline phase, the preservation of the SCO properties must also be assessed. Vibrating sample magnetometry (VSM) and differential scanning calorimetry (DSC) are particularly suitable techniques for this purpose. The complexes **Fe(L1)$_2$**, **Fe(L2)$_2$** and **Fe(L3$_2$)**, obtained via both solution-state and one-pot synthesis were analysed by VSM magnetometry to evaluate their SCO behaviour. **Figure 4** shows the effect of temperature on the high spin fraction (n_{HS}) for all three compounds synthesised using mechanochemical and solution-state methods. The $\chi_M T$ curves, as well as all transition temperatures and associated parameters, can be found in the ESI. For **Fe(L1)$_2$-sol,** the transition temperatures were determined as $T_{1/2\uparrow}$ = 287 K and $T_{1/2\downarrow}$ = 277 K, corresponding to a thermal hysteresis width of $\Delta T_{1/2}$ = 10 K (smoothness of 6 K), in good agreement with previous literature results.[21] In the case of **Fe(L1)$_2$-mech**, the spin transition is shifted to lower temperatures, with $T_{1/2\uparrow}$ = 282 K and $T_{1/2\downarrow}$ = 265 K, accompanied by a slight increase in the hysteresis width ($\Delta T_{1/2}$ = 17 K, smoothness of 6 K) (**Figure 4a**).
For **Fe(L2)$_2$-sol**, the transition temperatures were determined as $T_{1/2\uparrow}$ = 266 K and $T_{1/2\downarrow}$ = 263 K ($\Delta T_{1/2}$ = 3 K, smoothness of 10 K). In the case of **Fe(L2)$_2$-mech**, the spin transition is slightly more abrupt and shifted to lower temperatures, with $T_{1/2\uparrow}$ = 258 K and $T_{1/2\downarrow}$ = 253 K ($\Delta T_{1/2}$ = 5 K, smoothness of 9 K) (**Figure 4b).** For the **Fe(L3)$_2$-sol** and **Fe(L3)$_2$-mech** samples, both exhibit more gradual spin crossover behaviour. For **Fe(L3)$_2$-sol**, $T_{1/2}$ is 308 K (smoothness of 29 K). For **Fe(L3)$_2$-mech**, $T_{1/2}$ is 302 K, also very gradual with a smoothness increasing to 40 K (**Figure 4c**).
It is well established that the presence of abrupt transitions and large hysteresis width are due to the cooperativity of the system, which in turn depends on first- and second-neighbour interactions and is most effective in well-ordered crystalline materials. The mechanochemically-synthesised materials **Fe(L1)$_2$-mech** and **Fe(L2)$_2$-mech** show a significantly wider hysteresis and comparable abruptness to the solution-synthesized material. This is perhaps surprising given their smaller particle sizes, and suggests that milling enhances cooperative behaviour. In contrast, **Fe(L3)$_2$-mech** shows a **Table** gradual transition with increased smoothness, indicating reduced cooperativity.
In previous studies, reduced particle size has been shown to reduce hysteresis width in triazole-based coordination polymers[39,40] and bimetallic coordination frameworks[41,42], particularly as the size is reduced to the nanoscale. However, in molecular SCO materials, crystallinity of the particles has been shown to have a more significant impact on cooperativity than particle size or morphology.[37]
Another important effect of milling concerns the fraction of material participating in the SCO process, as indicated by the

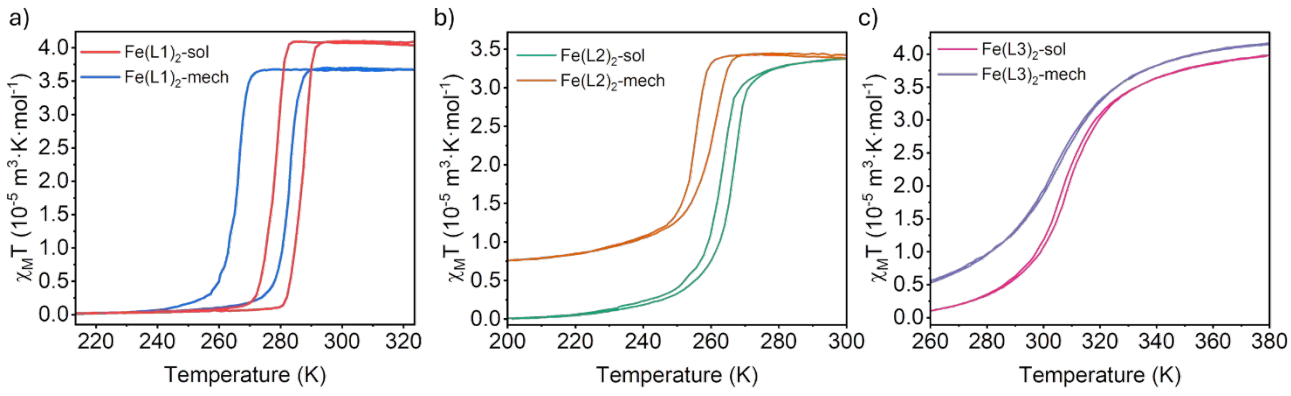

Figure 4. Temperature-dependent $\chi_M T$ for **Fe(L1)$_2$-sol** and **Fe(L1)$_2$-mech** (a), **Fe(L2)$_2$-sol** and **Fe(L2)$_2$-mech** (b), and **Fe(L3)$_2$-sol** and **Fe(L3)$_2$-mech** (c).

absolute $\chi_M T$ values. While **Fe(L1)$_2$-mech** shows a nearly complete transition, **Fe(L2)$_2$-mech** and **Fe(L3)$_2$-mech** display larger residual HS fractions than their solution-synthesised analogues, as reflected by their higher $\chi_M T$ values at low temperature. Previous studies have shown that mechanochemistry can induce such differences, attributed to partial recrystallization and the formation of a non-SCO, amorphous phase that is not detectable by PXRD.[43] In the case of **Fe(L1)$_2$**, there is a difference in the absolute $\chi_M T$ values in the HS state, between the two samples, which cannot be attributed to the presence of impurities. This aspect is currently under further investigation but is beyond the scope of this work.

The DSC measurements (Figs. S21–S23 and Tables S3–S6 in the ESI) further confirm the transition temperatures observed by VSM and highlight the differences between **Fe(L1)$_2$-sol** and **Fe(L1)$_2$-mech**. While the transition temperatures upon heating ($T_{1/2\uparrow}$) are very similar for both methods, a significant difference is observed in the transition temperatures upon cooling ($T_{1/2\downarrow}$), resulting in a wider thermal hysteresis for the mechanochemically synthesised material. For Fe(L1), the standard deviations of the transition temperatures are comparable for both synthetic methods. The increase in the hysteresis width in **Fe(L1)$_2$-mech** indicates increased cooperativity in the mechanochemically synthesised product, whereas the thermodynamic parameters indicate similar values arising from both synthetic methods. Combined with the apparent difference in $\chi_M T$ values in the HS states, this seems to indicate a subtle structural difference between solution and mechanochemically synthesised products, which in the light of the very similar diffractograms likely appears at the microstructure level.

In contrast, **Fe(L2)$_2$-mech** exhibits a similar hysteresis width regardless of **Fe(L2)$_2$-sol**, indicating that the degree of cooperativity is preserved. However, both the cooling and heating transition temperatures are shifted to lower values in the mechanochemically synthesised material, suggesting a stabilisation of the high-spin state relative to the solution-prepared analogue. Since the hysteresis is unaffected, this shift is more likely associated with changes in the thermodynamic balance between the high and low spin states than with variations in cooperativity. Such differences may arise from subtle changes in lattice energy, the presence of structural defects, or differences in the crystallinity of the material induced by the synthetic route.

Due to the gradual nature of the spin transition in **Fe(L3)$_2$**, no well-defined DSC peaks are observed, preventing reliable determination of the transition enthalpy and entropy for this compound.

Conclusions

In this work, we report a mechanochemical one-pot synthesis strategy that combines the condensation of hydrazones with aldehydes, deprotonation, and metal coordination reactions. Under the influence of mechanical forces, these processes drive the self-organization of the starting materials through synergistic interactions, sequentially generating the ligands via condensation, promoting their deprotonation, and ultimately enabling the formation of iron(II) complexes through complexation. Notably, the reaction reached complete conversion at a c.a. 1 g scale within just 10 minutes, highlighting the efficiency and sustainability of mechanochemical methods. The present results show that mechanochemical processing can modify the SCO behaviour, including the transition temperature and, in some cases, the abruptness of the transition. The observed shift of the SCO transitions towards lower temperatures suggests that this approach may be useful for expanding the range of accessible operating temperatures in known SCO systems. These findings may also motivate future studies exploring the potential of such materials for barocaloric applications, as mechanochemical synthesis could facilitate their scalable production, an important requirement for the practical implementation of barocaloric technologies. This one-pot mechanochemical approach not only streamlines the synthesis of Schiff-base complexes but also provides a promising platform for further investigating the structural factors that influence SCO behaviour and its modification across related systems. Overall, this study provides a clear demonstration of reaction pathways in one-pot synthesis and solid-state transformations, showcasing mechanochemistry as a green, fast, and effective strategy for the preparation of Schiff-base complexes and SCO compounds.

Author Contributions

YSA and CGD contributed equally to this work and share first authorship. YSA: methodology, investigation, formal analysis of synthetic processes and materials characterisation, writing – original draft. CGD: methodology, investigation, formal analysis of synthetic processes and materials characterisation, writing – original draft. AI: investigation, formal analysis of VSM data, writing – review and editing. FP: investigation, formal analysis of VSM data, writing – review and editing. PR: funding acquisition, supervision, writing – review and editing. HJS: conceptualisation, methodology, funding acquisition, supervision, writing – review and editing.

Data availability

The datasets supporting this work are available in Zenodo at https://zenodo.org/records/20731583. Raw experimental data and associated metadata, are available from this repository.

Conflicts of interest

The authors declare no conflicts of interests.

Acknowledgements

This work was performed in the context of Horizon Europe EIC Pathfinder Challenge project First Regenerative Solid-State

Barocaloric Refrigerator (FROSTBIT, Grant Agreement 101161137). UK participants in Horizon Europe Project First Regenerative Solid-State Barocaloric Refrigerator (FROSTBIT) are supported by UKRI grant number 10134597. Authors thank Dominick Balderston for technical assistance in data acquisition. The Low Temperature Physical Measurements and the Physico-Chemical Characterization (N. Daro) services at ICMCB are acknowledged for magnetometric measurements and elemental analyses.

Notes and references

1 P. Gütlich and H.A. Goodwin, *Spin Crossover in Transition Metal Compounds I*, Springer Berlin Heidelberg, Berlin, Heidelberg, 2004, vol. 233.

2 J. A. Real, A. B. Gaspar and M. C. Muñoz, Thermal, pressure and light switchable spin-crossover materials, *Dalton Transactions*, 2005, 2062–2079.

3 K. S. Murray, in *Spin-Crossover Materials*, 2013, pp. 1–54.

4 P. Gütlich, A. B. Gaspar and Y. Garcia, Spin state switching in iron coordination compounds, *Beilstein Journal of Organic Chemistry*, 2013, **9**, 342–391.

5 K. Senthil Kumar and M. Ruben, Emerging trends in spin crossover (SCO) based functional materials and devices, *Coord. Chem. Rev.*, 2017, **346**, 176–205.

6 W. Klaeui, W. Eberspach and P. Guetlich, Spin-crossover cobalt(III) complexes: steric and electronic control of spin state, *Inorg. Chem.*, 1987, **26**, 3977–3982.

7 S. Brooker, P. G. Plieger, B. Moubaraki and K. S. Murray, [CoII2L(NCS)2(SCN)2]: The First Cobalt Complex to Exhibit Both Exchange Coupling and Spin Crossover Effects, *Angew. Chem. Int. Ed.*, 1999, **38**, 408–410.

8 S. Hayami, Z. Gu, H. Yoshiki, A. Fujishima and O. Sato, Iron(III) Spin-Crossover Compounds with a Wide Apparent Thermal Hysteresis around Room Temperature, *J. Am. Chem. Soc.*, 2001, **123**, 11644–11650.

9 G. G. Morgan, K. D. Murnaghan, H. Müller-Bunz, V. McKee and C. J. Harding, A Manganese(III) Complex That Exhibits Spin Crossover Triggered by Geometric Tuning, *Angew. Chem. Int. Ed.*, 2006, **45**, 7192–7195.

10 Y.-C. Chuang, C.-T. Liu, C.-F. Sheu, W.-L. Ho, G.-H. Lee, C.-C. Wang and Y. Wang, New Iron(II) Spin Crossover Coordination Polymers [Fe(μ-atrz)3]X2·2H2O (X = $ClO4^-$, $BF4^-$) and [Fe(μ-atrz)(μ-pyz)(NCS)2]·4H2O with an Interesting Solvent Effect, *Inorg. Chem.*, 2012, **51**, 4663–4671.

11 T. Sugaya, T. Fujihara, T. Naka, T. Furubayashi, A. Matsushita, H. Isago and A. Nagasawa, Observation of the First Spin Crossover in an Iron(II) Complex with an S6 Coordination Environment: Tris[bis(N,N-diethylamino)carbeniumdithiocarboxylato]iron(II) Hexafluorophosphate, *Chemistry – A European Journal*, 2018, **24**, 17955–17963.

12 H. S. Scott, R. W. Staniland and P. E. Kruger, Spin crossover in homoleptic Fe(II) imidazolylimine complexes, *Coord. Chem. Rev.*, 2018, **362**, 24–43.

13 O. Kahn, Spin-crossover molecular materials, *Curr. Opin. Solid State Mater. Sci.*, 1996, **1**, 547–554.

14 A. Bousseksou and G. Molnár, The spin-crossover phenomenon: towards molecular memories, *Comptes Rendus Chimie*, 2003, **6**, 1175–1183.

15 S. Hayami, S. M. Holmes and M. A. Halcrow, Spin-state switches in molecular materials chemistry, *J. Mater. Chem. C Mater.*, 2015, **3**, 7775–7778.

16 M. D. Manrique-Juárez, S. Rat, L. Salmon, G. Molnár, C. M. Quintero, L. Nicu, H. J. Shepherd and A. Bousseksou, Switchable molecule-based materials for micro- and nanoscale actuating applications: Achievements and prospects, *Coord. Chem. Rev.*, 2016, **308**, 395–408.

17 S. P. Vallone, A. N. Tantillo, A. M. dos Santos, J. J. Molaison, R. Kulmaczewski, A. Chapoy, P. Ahmadi, M. A. Halcrow and K. G. Sandeman, Giant Barocaloric Effect at the Spin Crossover Transition of a Molecular Crystal, *Advanced Materials*, 2019, **31**, 1807334.

18 M. Romanini, Y. Wang, K. Gürpinar, G. Ornelas, P. Lloveras, Y. Zhang, W. Zheng, M. Barrio, A. Aznar, A. Gràcia-Condal, B. Emre, O. Atakol, C. Popescu, H. Zhang, Y. Long, L. Balicas, J. Lluís Tamarit, A. Planes, M. Shatruk and L. Mañosa, Giant and Reversible Barocaloric Effect in Trinuclear Spin-Crossover Complex Fe3(bntrz)6(tcnset)6, *Advanced Materials*, 2021, **33**, 2008076.

19 J. Seo, J. D. Braun, V. M. Dev and J. A. Mason, Driving Barocaloric Effects in a Molecular Spin-Crossover Complex at Low Pressures, *J. Am. Chem. Soc.*, 2022, **144**, 6493–6503.

20 T. Kuroda-Sowa, Z. Yu, Y. Senzaki, K. Sugimoto, M. Maekawa, M. Munakata, S. Hayami and Y. Maeda, Abrupt Spin Transitions and LIESST Effects Observed in FeII Spin-crossover Complexes with Extended π-Conjugated Schiff-base Ligands Having N4O2 Donor Sets, *Chem. Lett.*, 2008, **37**, 1216–1217.

21 L. Zhang, G.-C. Xu, H.-B. Xu, T. Zhang, Z.-M. Wang, M. Yuan and S. Gao, Abrupt spin transition around room temperature and light induced properties in FeII complexes with N4O2 coordination sphere, *Chemical Communications*, 2010, **46**, 2554–2556.

22 W. Phonsri, C. G. Davies, G. N. L. Jameson, B. Moubaraki, J. S. Ward, P. E. Kruger, G. Chastanet and K. S. Murray, Symmetry breaking above room temperature in an Fe(ii) spin crossover complex with an N4O2 donor set, *Chemical Communications*, 2017, **53**, 1374–1377.

23 W. Phonsri, D. S. Macedo, K. R. Vignesh, G. Rajaraman, C. G. Davies, G. N. L. Jameson, B. Moubaraki, J. S. Ward, P. E. Kruger, G. Chastanet and K. S. Murray, Halogen Substitution Effects on N2O Schiff Base Ligands in Unprecedented Abrupt FeII Spin Crossover Complexes, *Chemistry – A European Journal*, 2017, **23**, 7052–7065.

24 K. Senthil Kumar, Y. Bayeh, T. Gebretsadik, F. Elemo, M. Gebrezgiabher, M. Thomas and M. Ruben, Spin-crossover in iron(ii)-Schiff base complexes, *Dalton Transactions*, 2019, **48**, 15321–15337.

25 Economic and Social Committee and the Committee of the Regions. A New Industrial Strategy for Europe.

26 J. H. Askew and H. J. Shepherd, Mechanochemical synthesis of cooperative spin crossover materials, *Chemical Communications*, 2018, **54**, 180–183.

27 P. Guionneau, M. Marchivie, G. Bravic, J.-F. Létard and D. Chasseau, in *Spin Crossover in Transition Metal Compounds II Topics in Current Chemistry*, Springer Berlin Heidelberg, Berlin, Heidelberg, 2004, pp. 97–128.

28 H. Chen, Z. Guo, D. Feng, X. Jin and F. Guo, Mechanochemical one-pot synthesis and solid-state transformation of cobalt(ii) Schiff base complexes: a green route to tailored coordination architecture, *RSC Mechanochemistry*, 2025, **2**, 853–863.

29 T. E. Shaw, J. Arami, J.-F. Ayme, J.-M. Lehn and T. Jurca, Dynamic mechanochemistry: accelerated self-sorting of two imine-based metal complexes under solvent-free mechanochemical conditions, *RSC Mechanochemistry*, 2024, **1**, 33–37.

30 L. N. Ortiz-Trankina, J. Crain, C. Williams and J. Mack, Developing benign syntheses using ion pairs via solvent-free mechanochemistry, *Green Chemistry*, 2020, **22**, 3638–3642.

31 T. Yong, G. Báti, F. García and M. C. Stuparu, Mechanochemical transformation of planar polyarenes to curved fused-ring systems, *Nat. Commun.*, 2021, **12**, 5187.

32 J. Yang, X. Feng, G. Lu, Y. Li, C. Mao, Z. Wen and W. Yuan, NaCl as a solid solvent to assist the mechanochemical synthesis and post-synthesis of hierarchical porous MOFs with high I2 vapour uptake, *Dalton Transactions*, 2018, **47**, 5065–5071.

33 J. F. Reynes, F. Leon and F. García, Mechanochemistry for Organic and Inorganic Synthesis, *ACS Organic & Inorganic Au*, 2024, **4**, 432–470.

34 B. Shaabani, A. A. Khandar, H. Mobaiyen, N. Ramazani, S. S. Balula and L. Cunha-Silva, Novel pseudohalide-bridged Cu(II) complexes with a hydrazone ligand: Evaluation of antimicrobial activity, *Polyhedron*, 2014, **80**, 166–172.

35 S. Martin-Martínez, C. Morales-Manrique, G. Marín and D. Gamba-Sánchez, Mechanochemical sulfenylation of maleimides, *Green Chemistry*, 2026, **28**, 11162–11169.

36 H. J. Shepherd, G. Molnár, W. Nicolazzi, L. Salmon and A. Bousseksou, Spin Crossover at the Nanometre Scale, *Eur. J. Inorg. Chem.*, 2013, **2013**, 653–661.

37 F. J. Valverde-Muñoz, A. B. Gaspar, S. I. Shylin, V. Ksenofontov and J. A. Real, Synthesis of Nanocrystals and Particle Size Effects Studies on the Thermally Induced Spin Transition of the Model Spin Crossover Compound [Fe(phen)2(NCS)2], *Inorg. Chem.*, 2015, **54**, 7906–7914.

38 I. A. Gural'skiy, C. M. Quintero, G. Molnár, I. O. Fritsky, L. Salmon and A. Bousseksou, Synthesis of Spin-Crossover Nano- and Micro-objects in Homogeneous Media, *Chemistry – A European Journal*, 2012, **18**, 9946–9954.

39 J. R. Galán-Mascarós, E. Coronado, A. Forment-Aliaga, M. Monrabal-Capilla, E. Pinilla-Cienfuegos and M. Ceolin, Tuning Size and Thermal Hysteresis in Bistable Spin Crossover Nanoparticles, *Inorg. Chem.*, 2010, **49**, 5706–5714.

40 M. Giménez-Marqués, M. L. García-Sanz de Larrea and E. Coronado, Unravelling the chemical design of spin-crossover nanoparticles based on iron(ii)–triazole coordination polymers: towards a control of the spin transition, *J. Mater. Chem. C Mater.*, 2015, **3**, 7946–7953.

41 F. Volatron, L. Catala, E. Rivière, A. Gloter, O. Stéphan and T. Mallah, Spin-Crossover Coordination Nanoparticles, *Inorg. Chem.*, 2008, **47**, 6584–6586.

42 Y. Raza, F. Volatron, S. Moldovan, O. Ersen, V. Huc, C. Martini, F. Brisset, A. Gloter, O. Stéphan, A. Bousseksou, L. Catala and T. Mallah, Matrix-dependent cooperativity in spin crossover Fe(pyrazine)Pt(CN)4 nanoparticles, *Chemical Communications*, 2011, **47**, 11501–11503.

43 D. Nieto-Castro, F. A. Garcés-Pineda, A. Moneo-Corcuera, B. Pato-Doldan, F. Gispert-Guirado, J. Benet-Buchholz and J. R. Galán-Mascarós, Effect of Mechanochemical Recrystallization on the Thermal Hysteresis of 1D FeII-triazole Spin Crossover Polymers, *Inorg. Chem.*, 2020, **59**, 7953–7959.

The datasets supporting this work are available in Zenodo at https://zenodo.org/records/20731583. Raw experimental data and associated metadata, are available from this repository.